ChemComm

Accepted Manuscript

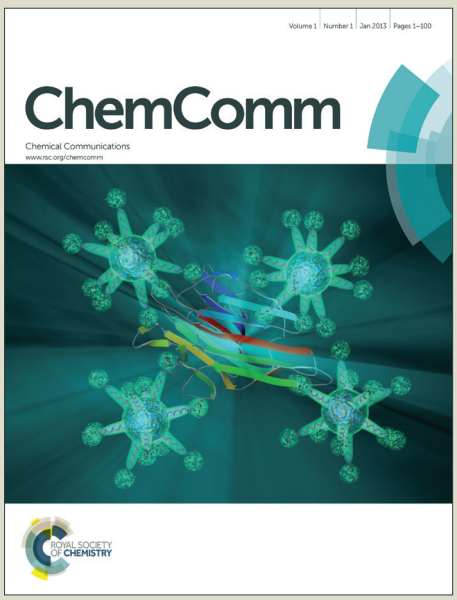

ROYAL SOCIETY OF CHEMISTRY

www.rsc.org/chemcomm

Chemical Communications

RSCPublishing

COMMUNICATION

Efficient delayed fluorescence from triplet-triplet annihilation for deep-blue electroluminescence

Cite this: DOI: 10.1039/xoxxoooooox

P.-Y. Chou,* [a] H.-H. Chou,[a] Y.-H. Chen,[a] T.-H. Su,[a] C.-Y. Liao,[a] H.-W. Lin[b], W.-C. Li [b], H.-Y. Yen,[a] I-C. Chen[a] and C.-H. Cheng*[a]

Received ooth January 2012,
Accepted ooth January 2012

DOI: 10.1039/xoxxoooooox

www.rsc.org/

Four 2-(styryl)triphenylene derivatives (TSs) were synthesized for deep-blue dopant materials. By using a pyrene-containing compound, DMPPP, as the host, the TSs-doped devices revealed significant delayed fluorescence via triplet-triplet annihilation, providing the highest quantum efficiency of 10.2% and current efficiency of 12.3 cd A^{-1}.

Recently, it has been reported that the performance limitation of fluorescent OLEDs can be overcome by the up-conversion of triplet to singlet states via two possible mechanisms, namely, thermally activated delayed fluorescence (TADF)[1] and triplet-triplet annihilation (TTA).[2,3] In the case of TADF, the small singlet-triplet energy gap (ΔE_{ST}) of the material enables triplet excitons to undergo reverse intersystem crossing to form singlet excitons. Although TADF materials can provide very high device efficiency, most TADF-based OLEDs show large efficiency roll-off and low device luminance.[1] Therefore, TTA materials with high EL efficiencies are considered to be potential candidates for practical use.

In this communication, we report four new deep-blue dopants containing 2-(styryl)triphenylene (TS) as the core moiety, including TSCz, TSTA, TSNA, and TSMA (Fig. 1). The deep-blue OLEDs fabricated using 1-(2,5-dimethyl-4-(1-pyrenyl)phenyl)pyrene (DMPPP) doped with one of the TSs as an emitting layer shows delayed electroluminescence and exhibits very high EL efficiencies with CIE_y less than 0.14. Enhanced by delayed fluorescence (DF), the device doped with TSTA shows the highest external quantum efficiency (EQE) of 10.2%, current efficiency of 12.3 cd A^{-1}, and luminance of 68,670 cd m^{-2}. The EQEs and current efficiencies of these doped OLEDs increased with increase in luminance, without compromising on the efficiency, owing to the increased TTA contribution at larger applied voltages.[3,4]

DMPPP, a pyrene-containing compound, (Fig. 1) has been used as a host material for fluorescent blue devices.[5] With the solid quantum efficiency (Φ_{PL}) of 0.85 and singlet energy gap of 3.2 eV, DMPPP is considered to be suitable as host for TSs-doped devices. The Φ_{PL}s of TSs in cyclohexane are near 0.90. However, the Φ_{PL}s of DMPPP films doped with 2% TSTA, TSNA, or TSMA were as high as 0.99 except that of the film doped with TSCz. In addition, a complete energy transfer of DMPPP excitons to TSTA leading to only TSTA emission was observed for the 2% TSTA/DMPPP film (Fig. S3). The high PL efficiencies of TSs in cyclohexane, the efficient energy transfer from DMPPP to TSs and the restricted rotation of the aromatic rings in the dopant and host molecules in the film that reduces the fluorescence quenching caused by rotation likely account for the very high Φ_{PL}s in the TS-doped thin films.[6] The UV absorption spectra of TSs in toluene and the photoluminescence (PL) spectrum of DMPPP are shown in Fig. S1. The maximum absorptions of TSs appear in the range of 350–400 nm, characteristic of π-π* transitions. Compared with TSCz, TSMA, TSTA, and TSNA show better overlap of the absorption spectra with the PL spectrum of DMPPP. This result plausibly accounts for the observed lower Φ_{PL} of the TSCz-doped DMPPP film. Further photophysical and thermal properties of TSs (see Fig. S1-4) were summarized in Table 1. In accordance with the high photoluminescence quantum efficiencies of DMPPP and TSs which lead to little or no intersystem crossing from singlet to triplet excited states, we were unable to measure their phosphorescent PL spectra at 77 K. Similarly, we measured the transient PLs of DMPPP film and of TSs in degassed toluene and no DF were observed for these compounds. These results exclude the possibility that DMPPP and TSs are TADF materials, in view of the fact that TADF material in general shows delayed fluorescence in the transient PL because the small ΔE_{ST} leads to the possibility of $T_1 \rightarrow S_1$ to produce DF.[1] The calculated HOMO and LUMO density maps of the TSs series (Fig. S5) also do not support that they are TADF materials.[1]

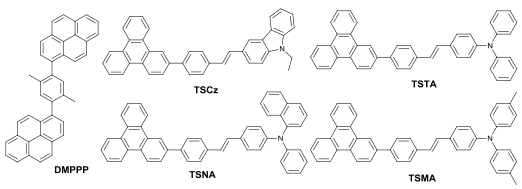

Fig. 1 Molecule structures of host and dopants

Subsequently, we fabricated OLEDs with the emission layer containing DMPPP doped with one of the TSs compounds, designated as A, B, C, and D, respectively. The device structure consists of ITO/NPNPB: 10% MoO_3 (5 nm)/NPNPB (80 nm)/NPB (10 nm)/DMPPP: 5% dopant (25 nm)/$BAlq_2$ (20 nm)/LiF (1 nm)/Al (100 nm). A thin layer of NPNPB (*N*,*N*′-di-phenyl-*N*,*N*′-di-[4-(*N*,*N*-di-phenyl-amino)pheny]benzidine) doped with 10% MoO_3 was used as the hole injection layer, in order to reduce the hole injection barrier.[7] All the devices fabricated in this study showed deep-blue EL emissions, with maximum peaks around 450 nm and $CIE_y \leq 0.14$ (Fig. S6). Fig. 2 shows the luminance dependence of the EQE and

Table 1. Photophysical and thermal properties of TSs

Compd	Abs_{sol} [a] (nm)	PL_{sol} [a] (nm)	PL_{film} [b] (nm)	HOMO[c], LUMO[d] (eV)	E_g [e] (eV)	T_g [f], T_d [g] (℃)	Φ_{PL} [h]
TSCz	358	420,442	469	5.37, 2.57	2.80	112, 431	0.85 (0.92)
TSTA	308, 386	441,462	470	5.38, 2.65	2.73	108, 431	0.89 (>0.99)
TSNA	386	441,462	469	5.38, 2.65	2.73	119, 448	0.90 (>0.99)
TSMA	308, 392	451	476	5.23, 2.53	2.70	100, 421	0.90 (0.99)

[a] Absorption and PL spectra measured in toluene with concentration = 1×10^{-5} M; [b] PL spectra measured in the thin film; [c] Determined by using a photoelectron spectrometer (AC-II); [d] LUMO = HOMO - E_g; [e] Band gaps were estimated from the optical absorption threshold in the films; [f] Glass-transition temperature determined by DSC with a heating rate of 20 ℃ min^{-1} under N_2; [g] Onset decomposition temperature, as measured with 5 % mass loss by TGA with a heating rate of 20 ℃ min^{-1} under N_2; [h] Fluorescence quantum efficiency, relative to 9,10-diphenylanthracene in cyclohexane (Φ_{PL} = 0.90); the data presented in the parentheses are the solid state photoluminescence quantum efficiency of the dopants in DMPPP thin film measured by an integral sphere with the excitation wavelength of 310 nm.

current efficiency of the devices. For device A, the EQE and current efficiency vs. luminance was nearly flat. On the other hand, the EQEs and current efficiencies of devices B, C, and D gradually increased with increase in luminance from 10 to 30,000 cd m^{-2}. These results are rather intriguing, as most OLED devices show obvious efficiency roll-off. Furthermore, devices B, C, and D exhibited very high EQEs of 10.2, 8.5 and 8.9%, respectively, and excellent current efficiencies of 12.3, 8.9 and 10.3 cd A^{-1}, respectively. It should be noted that the EQEs of all the four OLEDs fabricated in this study are much higher than the conventional upper limit of 5%. Furthermore, the operating lifetime of all the four OLEDs was tested under an initial luminance of 2,000 cd m^{-2} (Fig. S8). Device C showed the longest operation lifetime of about 210 h, which is projected to be about 680 h at 1000 cd m^{-2} according to the empirical lifetime acceleration function, $L_0^{1.7}\times t_{50} = const.$[8]

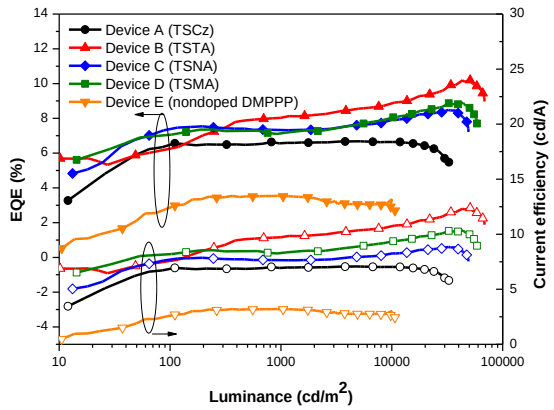

Fig. 2. EQEs and current efficiencies vs luminance for devices A-E.

To gain further insights on the observed unusually high efficiency of the doped blue devices, we also fabricated non-doped devices E and F with the same configuration as that of devices A-D, except only DMPPP and TSTA are used, respectively, in the emitting layer. Both devices E and F exhibited relatively low device efficiency compared with the doped devices (Table 2). It is likely that the high concentration of these molecules in the emitting layer leads to concentration-quenching and lowers the efficiency of these non-doped devices.[9] Subsequently, we measured the transient EL of devices A-F at 450 nm (Fig. 3a). As the decay lifetime of singlet excitons is generally within several ns, the results clearly show microsecond-scale DF for all devices including the non-doped devices E and F. These surprising results indicate that both DMPPP and dopants (TSs) are able to produce DF. We also measured the transient EL of the DMPPP-based devices doped with different concentrations of TSTA in the emitting layer, namely, 2, 5, 10, 15 and 100% (Fig. 3b). The results reveal that the dopant used and its

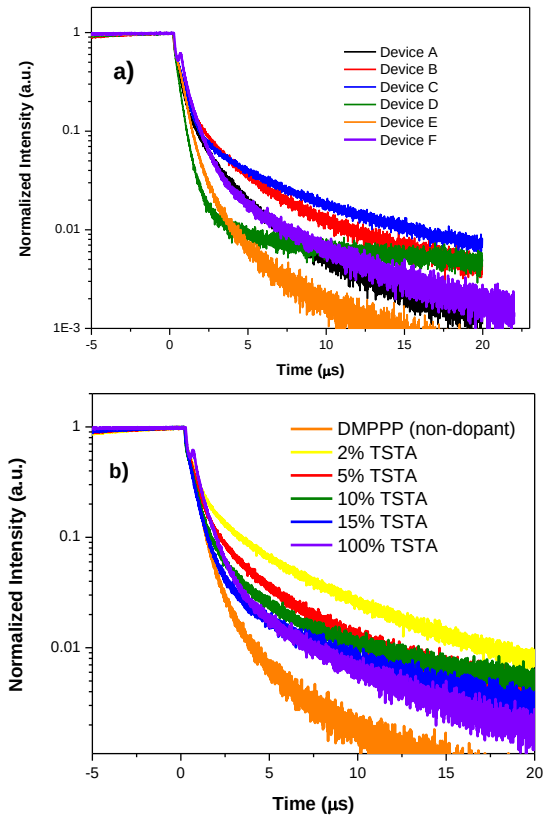

Fig. 3. a) Transient EL of devices A-F measured at 450 nm; b) Transient EL of the devices doped with different concentrationof TSTA (device structure is similar to device B except the concentration of TSTA) measured at 450 nm.

concentration influence the relative DF intensity significantly. As disclosed in Fig. 3b, the relative DF intensity of the TSTA-doped devices decreases with increasing TSTA concentration suggesting that a low TSTA concentration in DMPPP host gives relatively high DF intensity. Device B with an optimized TSTA/DMPPP ratio of 95/5 in the emitting layer does contain a substantial DF contribution of the EL intensity. To further understand the DF property of these EL devices, we tried to fit the transient EL curves in Fig. 3. A plot of the inverse of relative transient EL intensity vs time (between 5-15 μs) is linear for each transient EL curve (see Fig. S12 - S13 for the slopes). The results show that the transient EL decay is second-order to the EL intensity and a support that the DF of these devices is a TTA process ($T^1 + T^1 \rightarrow S^1 + S^0$) which is known to be second-order with respect to T^1 concentration.[4,10]

Table 2. Electroluminescence performance of devices A-F.

Device	EML[a]	V_{on}[b]	EQE[c]	η_c[d]	η_p[e]	L_{max}[f]	λ_{max}[g]	CIE(x, y)[h]	t_{50}[i]
A	5% TSCz	4.4	6.7 (10.6 V)	7.1 (10.6 V)	3.8 (5.2 V)	33510 (18.6 V)	448	0.15, 0.10	75
B	5% TSTA	3.8	10.2 (15.0 V)	12.3 (15.0 V)	5.7 (3.8 V)	68670 (18.2 V)	454	0.14, 0.14	100
C	5% TSNA	3.6	8.5 (14.2 V)	8.9 (14.2 V)	4.8 (4.6 V)	49060 (17.2 V)	450	0.14, 0.11	210
D	5% TSMA	3.4	8.9 (15.0 V)	10.3 (15.0 V)	8.7 (3.4 V)	58640 (18.0 V)	460	0.14, 0.14	35
E	DMPPP	4.8	3.5 (8.2 V)	3.2 (9.6 V)	1.3 (7.2 V)	10840 (18.0 V)	444	0.16, 0.10	-
F	TSTA	3.6	4.2 (7.0 V)	7.6 (7.0 V)	3.8 (5.0 V)	30584 (20.0 V)	470	0.14, 0.25	-

[a] Emission layer of devices A-F: DMPPP/5% dopant; [b] The voltage at 10 cd m^{-2} (V); [c] Maximum external quantum efficiency (%); [d] Maximum current efficiency (cd A^{-1}); [e] Maximum power efficiency (lm W^{-1}); [f] Maximum luminance (cd m^{-2}); [g] The electroluminescence wavelength (nm); [h] Recorded at 8 V; [i] Operation lifetime at initial luminance of 2,000 cd m^{-2} under constant current.

The delayed EL spectrum of TSTA-doped device B shows slightly red shifted compared with its device and prompt EL spectra (Fig. S9). Moreover, the delayed EL spectrum of the non-doped device E exhibits a much broader emission with a shoulder at 550 nm, which may be assigned as an excimer emission of DMPPP.[11] As a result, the relative delayed EL of device E (Fig. S10) measured at 550 nm is relatively stronger than at 450 nm. The evidences that support the observed DF in the present devices is TTA are further summarized below. One is the EQE vs luminance curve which shows an increase in efficiency for higher luminance (see Fig. 2).[4] The results agree well with the observed TTA phenomenon which is a second order process proportional to the square of the triplet-exciton concentration; we expected that the triplet excitons generated by the device is nearly proportional to the current density of the device. Similarly, the dependence of luminescence on current density as shown in Fig. S15 is a non-linear curve. The luminescence increased more than linearly with an increase in current density, a character of TTA-type devices.[12] The other evidence to support TTA is that the decay rate of the transient EL intensity is second-order with respect to the transient EL intensity (Fig. S12 - S13).

In summary, we have demonstrated that DMPPP/TSs-based devices are highly efficient affording the highest EQE of 10.2% and maximum current efficiency of 12.3 cd A^{-1}. Both DMPPP and TSs appear to exhibit TTA-type delayed EL. It is the first time that pyrene- and triphenylene-containing materials with TTA property were used in OLEDs. In contrast to the TADF-based OLEDs, which generally have low maximum luminance and high roll-off efficiencies, the present devices A–D provide very high luminance of 33510–68670 cd m^{-2} without compromising on the efficiency.

We thank the Ministry of Science and Technology of Republic of China (NSC-102-2633-M-007-002) for support of this research and National Center for High-Performance Computing (Account number: u32chc04) of Taiwan for providing the computing time.

Notes and references

[a] Department of Chemistry, National Tsing Hua University, Hsinchu 30013, Taiwan. E-mail chcheng@mx.nthu.edu.tw
[b] Department of Materials Science and Engineering, National Tsing Hua University, Hsinchu 30013, Taiwan.
Electronic Supplementary Information (ESI) available: general information, synthesis, ^{1}H and ^{13}C NMR spectra and photophysical, thermal and electroluminescence properties. See DOI: 10.1039/c000000x/

1 Q. Zhang, J. Li, K. Shizu, S, Huang, S. Hirata, H. Miyazaki and C. Adachi, *J. Am. Chem. Soc*. 2012, **134**, 14706; G. Méhes, H. Nomura, Q. Zhang, T. Nakagawa and C. Adachi, *Angew. Chem*. 2012, **51**, 11311; H. Uoyama, K. Goushi, K. Shizu, H. Nomura and C. Adachi, *Nature*, 2012, **492**, 234.

2 C.-J. Chiang, A. Kimyonok, M. K. Etherington, G. C. Griffiths, V. Jankus, F. Turksoy and A. P. Monkman, *Adv. Funct. Mater*. 2013, **23**, 739; V. Jankus, C.-J. Chiang, F. Dias and A. P. Monkman, *Adv. Mater*. 2013, **25**, 1455; S.-K. Kim, B. Yang, Y. Ma, J.-H. Lee and J.-W. Park, *J. Mater. Chem.* 2008, **18**, 3376; Q. Wang, I. W. H. Oswald, M. R. Perez, H. Jia, B. E. Gnade and M. A. Omary, *Adv. Funct. Mater*. 2013, **23**, 5420.

3 H. Fukagawa, T. Shimizu, N. Ohbe, S. Tokito, K. Tokumaru and H. Fujikake, *Org. Electron.* 2012, **13**, 1197.

4 R. C. Kwong, S. Sibley, T. Dubovoy, M. Baldo, S. R. Forrest and M. E. Thompson, *Chem. Mater*. 1999, **11**, 3709; Y.-J. Pu, G. Nakata, F. Satoh, H. Sasabe, D. Yokoyama and J. Kido, *Adv. Mater.* 2012, **24**, 1765.

5 K.-C. Wu, P.-J. Ku, C.-S. Lin, H.-T. Shih, F.-I. Wu, M.-J. Huang, J.-J. Lin, I-C. Chen and C.-H. Cheng, *Adv. Funct. Mater*. 2008, **18**, 67; S.-H. Lin, F.-I. Wu, H.-Y. Tsai, P.-Y. Chou, H.-H. Chou, C.-H. Cheng and R.-S. Liu, *J. Mater. Chem.* 2011, **21**, 8122; H.-H. Chou, Y.-H. Chen, H.-P. Hsu, W.-H. Chang, Y.-H. Chen and C.-H. Cheng, *Adv. Mater*. 2012, **24**, 5867.

6 Y. Hong, J. W. Y. Lama and B. Z. Tang, *Chem. Commun.*, 2009, 4332; W. Z. Yuan, Y Gong, S. Chen, X. Y. Shen, J. W. Y. Lam, P. Lu, Y. Lu, Z. Wang, R. Hu, N. Xie, H. S. Kwok, Y. Zhang, J. Z. Sun and B. Z. Tang, *Chem. Mater.*, 2012, **24**, 1518.

7 F. Wang, X. Qiao, T. Xiong and D. Ma, *Org. Electron*. 2008, **9**, 985; J. Meyer, S. Hamwi, M. Kröger, W. Kowalsky, T. Riedl and A. Kahn, *Adv. Mater*. 2012, **24**, 5408.

8 C. Féry, B. Racine, D. Vaufrey, H. Doyeux and S. Cinà, *Appl. Phys. Lett.* 2005, **87**, 213502; G. Li, T. Fleetham and J. Li, *Adv. Mater*. 2014, DOI: 10.1002/adma.201305507.

9 C. W. Tang, S. A. Van Slyke and C. H. Chen, *J. Appl. Phys.*, 1989, **65**, 3610; M. Zhu and C. Yang, *Chem.Soc.Rev.*, 2013, **42**, 4963.

10 D. Y. Kondakov, T. D. Pawlik, T. K. Hatwar and J. P. Spindler, *J. Appl. Phys*., 2009, **106**, 124510.

11 W. Zhao and F. N. Castellano, *J. Phys. Chem. A.* 2006, **110**, 11440.

12 C. Ganzorig and M. Fujihira, *Appl. Phys. Lett*., 2002, **81**, 3137; C.-G. Zhen, Y.-F. Dai, W.-J. Zeng, Z. Ma, Z.-K. Chen and J. Kieffer, *Adv. Funct. Mater*. 2011, **21**, 699.